Molecular and Crystal Structures of Novel Second-Order Nonlinear Optical Crystals: α,α'-Dibenzylidenecycloalkanones

Jun Kawamata,* Kuon Inoue, and Tamotsu Inabe†

Research Institute for Electronic Science, Hokkaido University, Kita-ku, Sapporo 060

†Division of Chemistry, Graduate School of Science, Hokkaido University, Kita-ku, Sapporo 060

(Received April 27, 1998)

X-Ray crystallographic analyses have been performed for the crystals of α,α'-dibenzylidenecycloalkanone (DBCA) derivatives which preferentially crystallize in non-centrosymmetric space groups and become second-order nonlinear optical crystals. We examined the obtained structures while paying attention to the intermolecular short contacts common to their structure. As a result, relatively short C–H···O contacts between the cycloalkanone rings were found for 8 out of 10 DBCA derivatives. The C–H···O distances for all cyclopentanone derivatives are almost the same as the sum of the van der Waals radius of carbon and that of oxygen; also, the geometrical characteristics found from the C–H···O contacts are consistent with the C–H···O hydrogen bond. The derivatives form a non-centrosymmetric one-dimensional chain with this contact. Their non-centrosymmetric crystal structures are led not only by their molecular shape, but also by this C–H···O interaction.

Recently, organic materials with a large macroscopic second-order nonlinear optical susceptibility ($\chi^{(2)}$) have attracted much interest in view of their potential applicability in nonlinear optics and optoelectronics.[1,2] In order to develop an efficient second-order nonlinear optical organic crystal, it is necessary for a comprising molecule to possess large second-order molecular hyperpolarizability (β).[1] It is rather easy to predict the magnitude of β for a given molecule.[1] However, in addition to that, the molecule is required to crystallize in a non-centrosymmetric form so as not to cancel out an induced hyper-polarization. Since it is quite difficult to predict how a given molecule crystallizes in the lattice,[3] the requirement is a major impediment when attempting to engineer a material with a large $\chi^{(2)}$ coefficient.

It is well known that a molecule with a strong intramolecular charge-transfer system exhibits a large β (Ref. 1), and thus, almost all SHG (second-harmonic generation) organic crystals studied up until now have been derivatives of *p*-nitroaniline. However, the derivatives are not advantageous for applications because of their volatility and highly hygroscopic character.[4] Taking a variety of organic materials into consideration, we tried to find another intramolecular charge-transfer backbone which also exhibits a large β. According to Oudar's equation,[5] a molecule with a large absorption coefficient (ε) should exhibit a large β. The value of ε for acetophenone is reported to be 13000, whereas that of nitrobenzene is 10000.[6] This fact indicates that a molecule comprising a keto-group conjugated with aromatic rings has the possibility of exhibiting a large β. Therefore, we have undertaken the design of such ketone derivatives.

As mentioned above, the next problem is how to find the means to crystallize the derivative in a non-centrosymmetric form. According to the closed-packing theory,[7] molecular crystals have a tendency to crystallize with maximum density and minimum free volume.[3] Therefore, we have attempted to design bent-shaped molecules, which are expected to be arranged in a non-centrosymmetric form, by adjusting their bent shape. Recently, that utilizing a bent molecule is effective for engineering a second-order nonlinear optical organic material has also been reported by another group.[8] For the bent-shaped keto derivatives, we have adopted a series of α,α'-dibenzylidenecycloalkanones (DBCAs, Fig. 1).[9—11] As a result, we have found that they preferentially crystallize in a non-centrosymmetric space group, and that some of them are promising SHG crystals.[9] For example, a single crystal of 4-*t*-butyl-2,6-bis(*p*-methylbenzylidene)cyclohexanone (MBBCH) is found to exhibit a large phase-matching second-order nonlinear coefficient of 12 pm/V at 1.06 μm,[10] and powdered crystals of 2,5-bis(*p*-methylbenzylidene)cyclopentanone (MBCP) are found to exhibit a large effective second-order nonlinear coefficient of 57 pm/V at 1.06 μm.[11]

Our previous X-ray crystallographic analyses[10,11] have already revealed that the molecular shapes of cyclohexanone and cycloheptanone derivatives are indeed of a bent form, since the central cycloalkanone ring is twisted. However, the cyclopentanone derivatives were found to be almost planar in shape. A slight bending feature along the molecular plane was found only when a 2,5-dibenzylidenecyclopentanone (DBCP) derivative had substituents at the *p*-position of the terminal phenyl rings. Despite the molecular shape, the probability of finding SHG active (non-centrosymmetric) crystals for the DBCP derivatives was also anomalously high.[9] This fact suggests that something other than the molecular shape should also contribute to determining the molecular arrange-

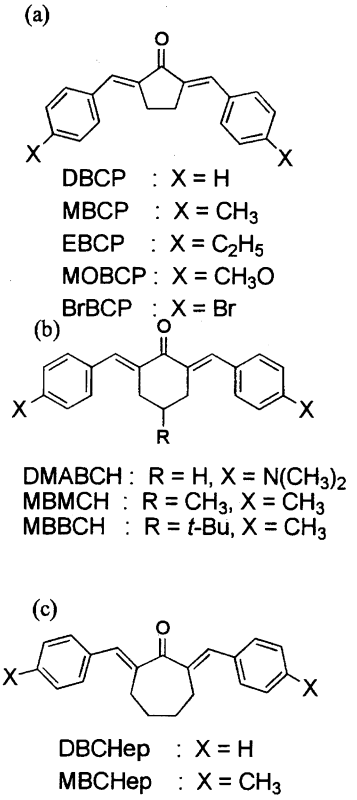

Fig. 1. Molecular structures of 2,5-dibenzylidenecyclopentanone (DBCP; (a)), 4-alkyl-2,6-dibenzylidenecyclohexanone (DBCH; (b)), and 2,7-dibenzylidenecycloheptanone (DBCHep; (c)) derivatives.

ment of the DBCP derivatives. Therefore, an X-ray crystallographic study has been systematically made in order to investigate any common crystallographic feature of DBCA derivatives. As a result, relatively short C–H···O contacts between the cycloalkanone rings have been found to be in common. In this paper we describe that the crystal structures of the present DBCA derivatives are led not only by their molecular shape, but also by this C–H···O interaction.

Experimental

Materials. A series of DBCAs investigated in the present work were synthesized in the same way as that reported in our previous paper.[9]

Measurements. The SHG intensity of the synthesized sample was estimated at 1.06 μm wavelength by means of the conventional powder method.[12] A pulsed beam from a repetitively Q-switched Nd-YAG laser was used for excitation. The particle size dependence of the signal intensity was measured over a range of from 20 to 150 μm in average diameter. No strong dependence of the signal intensity on particle size beyond 100 μm was observed for all of the samples examined. The SHG intensity reported in this paper refers to the value measured for a sufficiently large particle size, i.e., 150 μm in diameter, relative to that of urea at the same average size.

The melting point was determined from a calorimetric curve observed by using a differential scanning calorimeter at a heating rate of 5 K min^{-1}.

The cutoff wavelength was determined from the absorption spectrum for a methanol solution as such a value extrapolated from the steepest tangent to the abscissa in the absorbance curve.

X-Ray Structure Analyses. The X-ray crystallographic measurements for DBCP, MBCP, 2,5-bis(4-methoxybenzylidene)cyclopentanone (MOBCP), 2,5-bis(4-bromobenzylidene)cyclopentanone (BrBCP), 2,5-bis(4-ethylbenzylidene)cyclopentanone (EBCP), MBBCH, 2,6-bis(4-dimethylaminobenzylidene)cyclohexanone (DMABCH), 2,7-dibenzylidenecycloheptanone (DBCHep), and 2,7-bis(4-methylbenzylidene)cycloheptanone (MBCHep) were made using an automated Rigaku AFC-5R or AFC-7R diffractometer equipped with a graphite-monochromatized Mo $K\alpha$ radiation source (λ = 0.71073 Å). As for 4-methyl-2,6-bis(4-methylbenzylidene)cyclohexanone (MBMCH; **2a**), it was made using an automated Mac Science MXC18 diffractometer with the same radiation source. Data were collected at room temperature. In both cases twenty-five reflections within $20° < 2\theta < 30°$ were used to determine the lattice parameters. The determined crystal structures were solved by direct methods of SHELX 86,[13] SIR 92,[14] and DIRDIF.[15] A block-diagonal (UNICS III[16]) or full-matrix (Texan, Crystan GM) least-squares technique with anisotropic thermal parameters for non-hydrogen atoms and calculated hydrogen positions with isotropic thermal parameters (not refined for MBCP and MBMCH) was employed for a structure refinement. The thus-obtained crystallographic data are summarized in Table 1. The atomic coordinates and thermal parameters of non-hydrogen atoms, atomic coordinates and temperature factors of hydrogen atoms, and the $F_o - F_c$ tables are deposited as Document No. 71060 at the Office of the Editor of Bull. Chem. Soc. Jpn.

Results and Discussion

Substitution Effects. For a series of DBCP derivatives (Fig. 1a), we have synthesized a number of analogues equipped with various substituents at various positions. Their SHG intensities are tabulated in Table 2a together with their melting points. We also synthesized some cyclopentanone derivatives equipped with other aromatics replacing the benzene ring; their SHG intensities are tabulated in Table 2b. The probability of finding SHG-active analogues was 67% (5/9) for *p*-substituted DBCPs and dicinnamylidenecyclopentanone derivatives, whereas those for *o*- or *m*-substituted DBCPs and poly-substituted derivatives were 13 (1/8) and 9% (1/11), respectively. From these data, it can be seen that *m*-, *o*-, and poly-substituted derivatives were essentially SHG-inactive. Thus, it may be possible to conclude that the DBCP derivative, which has a linear lateral moiety, generally exhibits SHG activity.

To consider the effect of replacing the central cycloalkanone ring, we examined 2,6-dibenzylidenecyclohexanone (DBCH) derivatives (Fig. 1b) and DBCHep derivatives (Fig. 1c). The results are given in Tables 3 and 4.

X-Ray Crystallographic Analyses for DBCAs. As mentioned above, SHG active DBCA crystals were composed of molecules equipped with linear lateral moieties. We thus performed X-ray analyses for DBCAs equipped with *p*-substituted benzylidene moieties. As examples of SHG-active analogues, we analyzed DBCP, MBCP, MOBCP, BrBCP, MBMCH, MBBCH, DMABCH, DBCHep, and MBCHep. As for an SHG inactive analogue, EBCP was also analyzed.

We examined the obtained structures while paying attention to the intermolecular short contacts common to their

Table 1. Crystallographic Data and X-Ray Experimental Details for DBCAs

Compound	DBCP	MBCP	MOBCP	BrBCP	EBCP
Formula	$C_{19}H_{16}O$	$C_{21}H_{20}O$	$C_{21}H_{20}O_3$	$C_{19}H_{14}OBr_2$	$C_{23}H_{24}O$
Formula weight	260.3	288.4	320.4	418.1	316.4
Crystal system	Orthorhombic	Orthorhombic	Orthorhombic	Orthorhombic	Monoclinic
Space group symmetry	$C222_1$	$Pca2_1$	$Cmc2_1$	$Abm2$	$C2/c$
Cell dimension					
a/Å	11.808(3)	14.901(9)	36.876(5)	7.259(2)	30.667(4)
b/Å	5.702(1)	18.170(9)	7.260(1)	36.996(12)	6.093(2)
c/Å	20.884(12)	6.002(5)	6.250(1)	6.038(1)	19.861(2)
β/°					97.536(11)
V/Å^3	1406.1(9)	1625.0(18)	1673.2(3)	1621.5(7)	3679.1(15)
Z	4	4	4	4	8
Number of independent molecule	0.5	1	0.5	0.5	1
Temperature/°C	23	23	23	23	23
Calculated density/g cm^{-3}	1.230	1.179	1.272	1.713	1.143
Maximum 2θ	50	60	50	50	50
Crystal size/mm	$0.2\times0.3\times0.3$	$0.05\times0.2\times0.4$	$0.25\times0.3\times0.35$	$0.2\times0.25\times0.35$	$0.15\times0.25\times0.4$
No. of reflections measured	2824	2672	8264	5937	4102
No. of reflections	656	864	2148	923	1611
used in refinement	$F_o > 3\sigma(F_o)$	$I_o > 2\sigma(I_o)$	$F_o > 3\sigma(F_o)$	$F_o > 3\sigma(F_o)$	$F_o > 3\sigma(F_o)$
No. of parameters	103	199	123	111	242
R	0.051	0.051	0.057	0.052	0.091
R_w	0.062	0.025	0.068	0.052	0.085

Compound	MBMCH	MBBCH	DMABCH	DBCHep	MBCHep
Formula	$C_{23}H_{24}O$	$C_{26}H_{30}O$	$C_{24}H_{28}N_2O$	$C_{21}H_{20}O$	$C_{23}H_{24}O$
Formula weight	316.4	358.5	360.5	288.4	316.4
Crystal system	Monoclinic	Orthorhombic	Orthorhombic	Monoclinic	Monoclinic
Space group symmetry	$P2_1$	$Pnm2_1$	$Pca2_1$	Pc	$P2_1$
Cell dimension					
a/Å	11.332(4)	7.849(1)	9.291(3)	8.095(1)	5.197(5)
b/Å	8.067(4)	23.428(3)	21.838(3)	5.954(1)	21.248(3)
c/Å	11.312(4)	5.942(1)	9.647(3)	17.512(2)	16.022(3)
β/°	119.2(3)			104.06(1)	94.09(3)
V/Å^3	902.7(6)	1042.5(2)	1957.4(8)	801.9(2)	1764.6(16)
Z	2	2	4	2	4
Number of independent molecule	1	0.5	1	1	2
Temperature/°C	23	23	23	23	23
Calculated density/g cm^{-3}	1.164	1.142	1.223	1.194	1.191
Maximum 2θ	60	60	60	60	60
Crystal size/mm	$0.25\times0.35\times0.4$	$0.25\times0.35\times0.35$	$0.2\times0.3\times0.3$	$0.2\times0.2\times0.35$	$0.15\times0.25\times0.3$
No. of reflections measured	2928	1816	1636	10276	5149
No. of reflections	1926	1207	1233	4256	1895
used in refinement	$I_o > 2\sigma(I_o)$	$F_o > 3\sigma(F_o)$	$F_o > 3\sigma(F_o)$	$F_o > 3\sigma(F_o)$	$F_o > 3\sigma(F_o)$
No. of parameters	217	147	273	220	482
R	0.070	0.057	0.060	0.057	0.099
R_w	0.090	0.065	0.061	0.066	0.073

Table 2. a. SHG Intensities by Means of Kurtz Method (×Urea) for a Series of DBCP Equipped with Various Substituents at the Terminal Phenyl Groups
Melting points (°C) are also shown in parentheses.

Substituent	*o*-	*m*-	*p*-
H			12 (198)
CH_3	0 (109)	0 (158)	30 (243)
CH_3O	0 (145)	0 (173)	19 (214)
Cl	0 (156)	0.2 (177)	0 (216)
Br	0 (167)	0 (186)	20 (252)
C_2H_5			0 (195)

	2,3-	2,4-	2,5-	2,6-	3,4-
di-Cl	0 (214)	0 (218)		0 (191)	
di-CH_3		0 (140)	0 (146)		
di-CH_3O	0 (143)	0 (187)	2.3 (185)		0 (198)

	2,3,4-	3,4,5-
tri-CH_3O	0 (158)	0 (207)

b. SHG Intensities (× Urea) and Melting Point (°C) of Some Analogues of DBCP Equipped with Another Aromatic Moiety at the Benzene Ring

Lateral group	SHG intensity	Melting point
1-Naphtylmethylene	0.2	186
2-Naphtylmethylene	2.3	279
Anthranylmethylene	0.2	> 300 (decomp)
Cinnamylidene	26	228
1-Methyl-3-phenyl-2-propenylidene	1.4	190

Table 3. SHG Intensities (×Urea) by Means of Kurtz Method for a Series of *p*-Substituted DBCP Derivatives
Melting points (°C) are also shown in parentheses.

Substituent	
H	0 (123)
CH_3	0.8 (168)
C_2H_5	7.7 (127)
n-C_3H_7	5.3 (153)
CH_3O	0 (160)
C_2H_5O	10 (151)
n-C_3H_7O	18 (123)
Cl	0 (149)
Br	0.6 (170)
$N(CH_3)_2$	50 (151)

structures. As a result, we found the formation of one-dimensional chains, of which the boundaries are drawn by thick solid lines in Figs. 2, 3, 4, 5, and 6. The chain is formed through a C–H···O intermolecular interaction, which is composed of C(3) carbon and carbonyl oxygen of the neighboring molecule. The interaction is shown by the hashed lines.

The C–H···O hydrogen bond[17] is a current topic concerning the factors which govern the molecular arrangement in the lattice. A broad survey by Desiraju[18,19] revealed that this interaction can be found in many crystals, and that it can be used for crystal design. The bond angle of the intermolecular C–H···O hydrogen bond was reported to be in the range 120—180°,[18,19] and the H···O=C angle for a carbonyl acceptor to be about 120°.[19,20] As shown in Table 5, the corresponding angles evaluated for the DBCA derivatives were found to be consistent with the above-mentioned ranges. It is also recognized that the existence of the C–H···O hydrogen bond raises the melting temperature.[21] Actually, the melting point of DBCP (198 °C) is considerably higher compared with related compounds which have a smaller number of C–H···O contacts, such as 1,5-diphenyl-1,4-pentadien-3-one[22] (no C–H···O contact; 107 °C) and DBCPM[23] (2-benzyl-5-benzylidenecyclopentanone, one C–H···O contact; 127 °C). In addition, it has recently been reported that DBCP can form a C–H···O hydrogen bond including the C(3) carbon

Table 4. SHG Intensities (×Urea) by Means of Kurtz Method for a Series of *p*-Substituted DBCH Equipped with Alkyl Group at the 4-Position of Central Cycloalkanone Ring and DBCHep
Melting points (°C) are also shown in parentheses.

Substituent	DBCH(4-Me)	DBCH(4-Et)	DBCH(4-*t*-Bu)	DBCHep
H	0 (101)	10 (91)	2.8 (145)	3.6 (108)
CH_3	25 (137)	0 (128)	23 (157)	16 (130)
CH_3O	2.1 (146)	18 (141)	20 (175)	0 (128)
C_2H_5	—	—	—	3.9 (101)

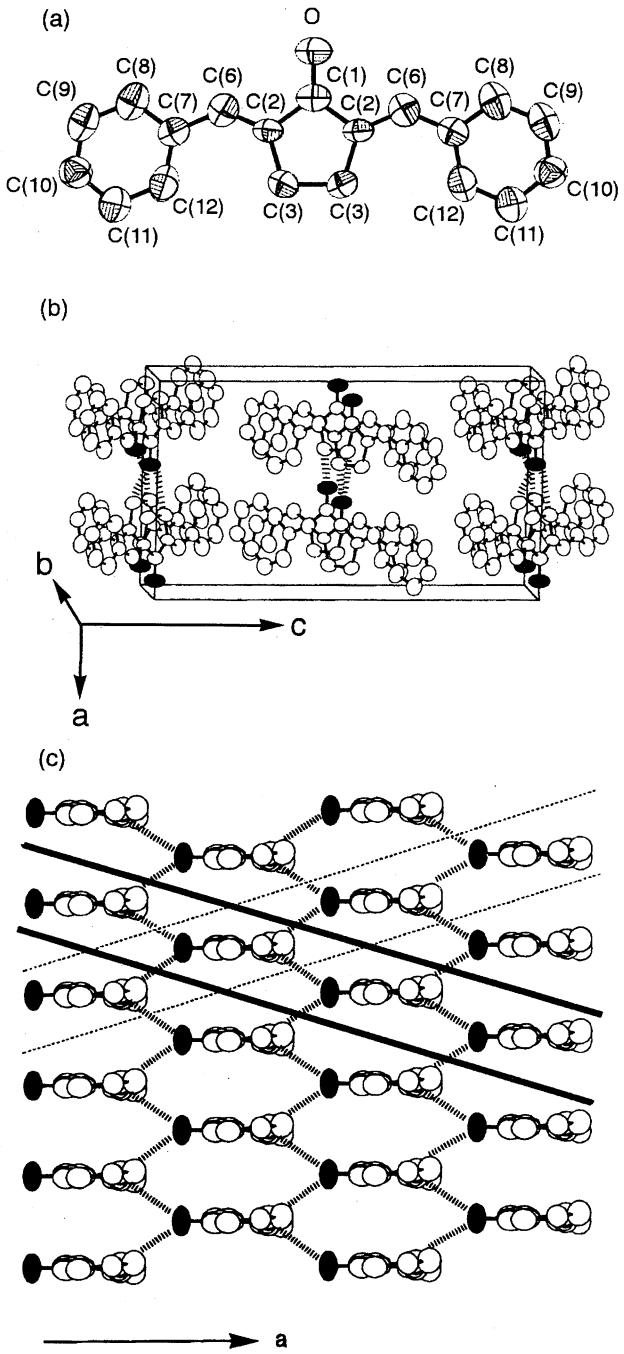

Fig. 2. ORTEP drawings of DBCP molecule showing the atom numbering scheme (a), and the crystal structure; view along the *b*-axis (b), view along the *c*-axis (c; molecules located within $-0.25 < z < 0.25$). The nearest contact between the carbonyl oxygen and neighboring molecules are drawn by hashed lines. Resulting one-dimensional chains are enclosed by thick solid and dotted lines.

in the 1 : 2 molecular complex with 1,3,5-trinitrobenzene.[24] Therefore, the C(3)–H···O interaction found in DBCAs is considered to be a kind of C–H···O hydrogen bond.

I. DBCP. As can be seen in Fig. 2c, two kinds of one-dimensional chains are defined. Each chain is enclosed by solid lines and dotted lines. Since the chains are crystallographically equivalent to each other, the architecture is

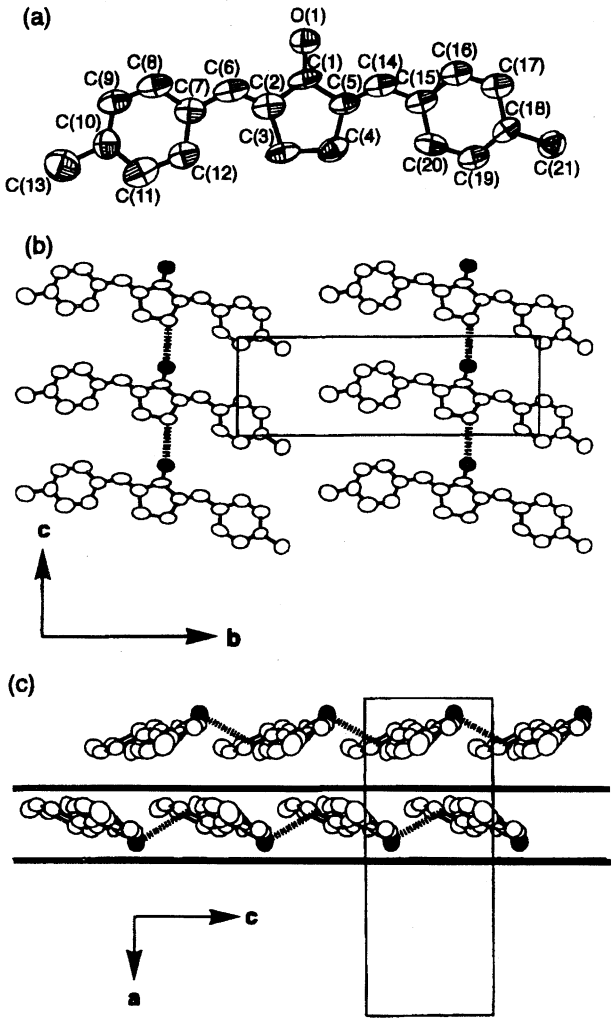

Fig. 3. ORTEP drawings of MBCP molecule showing the atom numbering scheme (a), and unit cell drawing; viewed along the *a*-axis (b; molecules located within $0 < x < 0.25$) and view along the *b*-axis (c). The nearest contact between the carbonyl oxygen and neighboring molecule is drawn by hashed lines. Resulting one-dimensional chain is enclosed by thick solid lines.

Table 5. Angles Evaluated for the C–H···O=C Contacts

Compound	C–H[a)]···O angle	H[a)]···O=C angle
	degree	degree
DBCP	149	143
MBCP	132	112
EBCP	132	127
MOBCP	130	136
BrBCP	128	127
MBBCH	149	109
DMABCH	144	99
DBCHep	129	124

a) Coordinates of the hydrogen atoms are calculated based on the ideal sp^3 carbon.

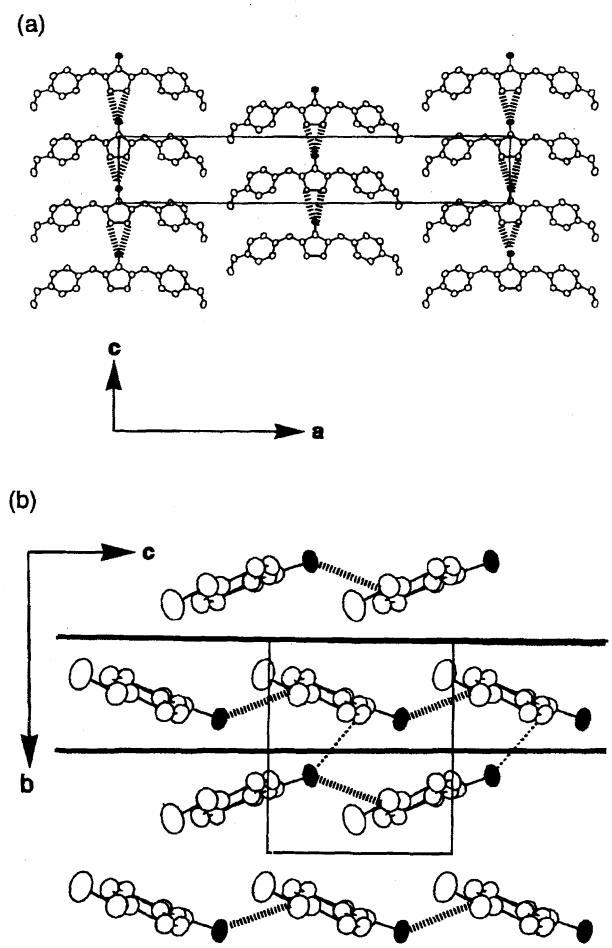

Fig. 4. Crystal structure of MOBCP; view along the *b*-axis (a; molecules located within $0 < y < 0.5$) and view along the *a*-axis (b; molecules located within $-0.25 < x < 0.25$). The nearest contact between the carbonyl oxygen and neighboring molecule is drawn by hashed lines. Resulting one-dimensional chain is enclosed by thick solid lines. Additional electrostatic interaction is drawn by dotted lines.

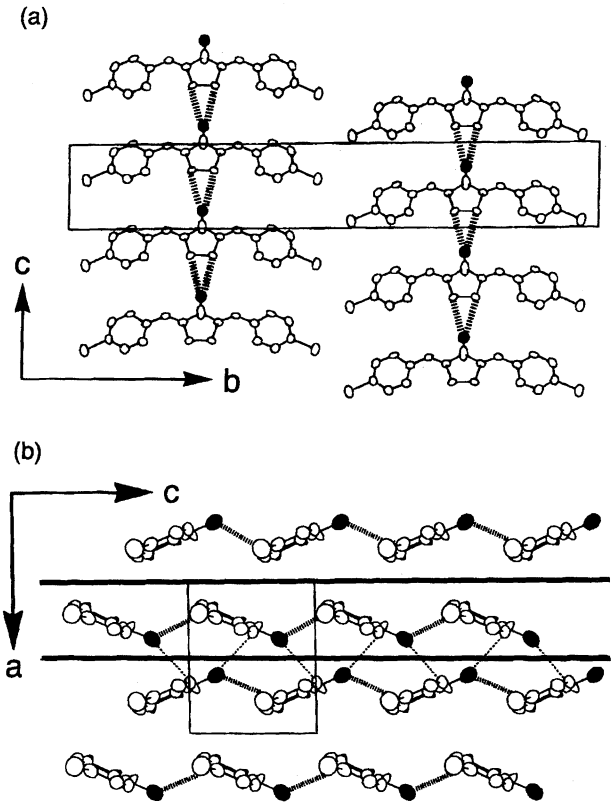

Fig. 5. Crystal structure of BrBCP; view along the *a*-axis (a; molecules located within $0 < x < 0.5$) and view along the *b*-axis (b; molecules located within $0 < y < 0.5$). The nearest contact between the carbonyl oxygen and neighboring molecule is drawn by hashed lines. Resulting one-dimensional chain is enclosed by thick solid lines. Additional electrostatic interaction is drawn by dotted lines.

actually a sheet. All of the carbonyl groups are aligned in the same direction within the sheet. However, as shown in Fig. 2b, the molecules in the neighboring sheets related by the two-fold axis align in an anti-parallel way. The net dipole moment is, however, not completely canceled out, since the component parallel to the two-fold axis survives.

II. MBCP. Two one-dimensional chains are found to be stacked up through the *c* glide plane, which is perpendicular to the *a*-axis and located at $x = 1/4$ and 3/4 (Fig. 3c). These double-chain units were packed in the lattice so as to be related by the two fold screw axis at (0, 0, *z*) and (1/2, 0, *z*). In this structure, all of the carbonyl dipoles are oriented in nearly the same direction.

III. MOBCP. The one-dimensional chain enclosed by the solid lines in Fig. 4b is stacked up with a neighboring chain through the *c* glide plane, which is perpendicular to the *b*-axis and located at $y = 1/2$, forming a double-chain unit. Our preliminary molecular-orbital calculation revealed that the C(1) carbon atom has a positive charge and the carbonyl oxygen atom has a negative charge. Therefore, it is considered that an additional electrostatic interaction, indicated by the dotted lines, operates between the O atom and the C(1) atom.

IV. BrBCP. As shown in Fig. 5, the characteristics found in the crystal structure of BrBCP are the same with those of MOBCP. Namely, a double-chain unit is formed by the *c* glide plane. An additional electrostatic interaction has also been found to be involved in Fig. 5b (drawn by dotted lines).

V. EBCP. The formation of the one-dimensional chain is also found in the crystal structure of EBCP (Fig. 6). The alignment of the chains resembles that of MBCP; in other words, the formation of a double-chain unit is also observed. Thus, the crystallographic characteristics of EBCP are essentially the same as those of other DBCP derivatives. However, the double-chain units are packed in such a way as to have an inversion center in the lattice. As a consequence, the EBCP crystal does not exhibit second-order optical nonlinearity.

VI. DBCH Derivatives. The formation of a one-dimensional chain is also found in the structures of DMABCH and MBBCH (Figs. 7c and 7d). However, a one-dimensional chain is not found in MBMCH (Fig. 7e).

VII. DBCHep Derivatives. The intermolecular

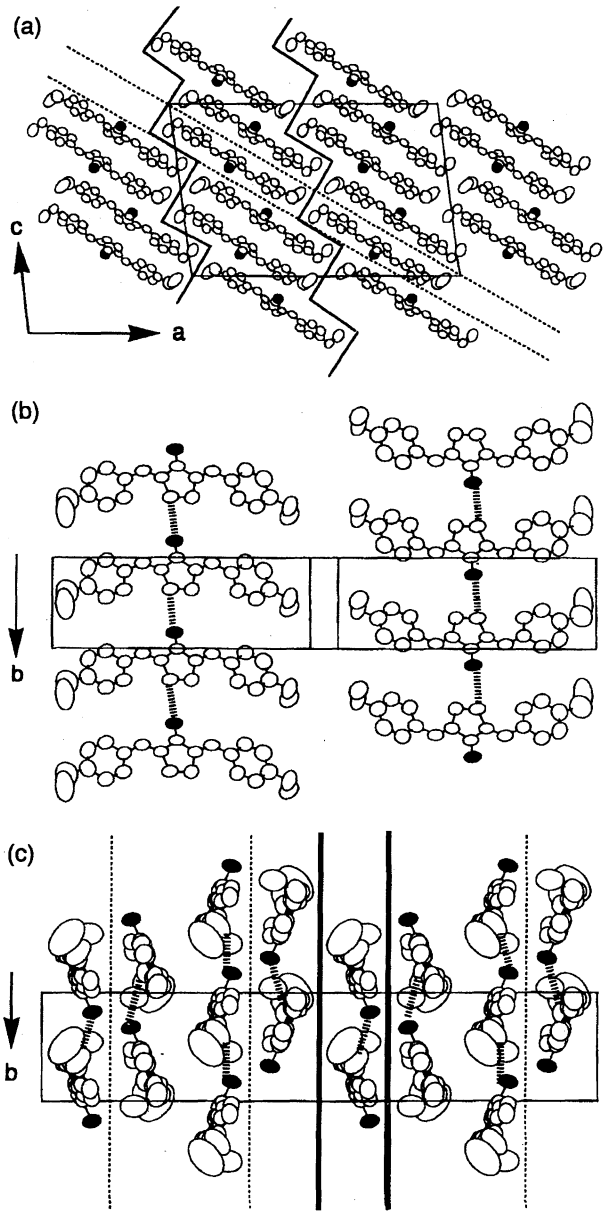

Fig. 6. Crystal structure of EBCP; view along the *b*-axis (a), view perpendicular to the (101) plane (b; molecules enclosed by dashed lines in (a)), and view parallel to the (101) plane (c; molecules enclosed by solid lines in (a)). The nearest contact between the carbonyl oxygen and neighboring molecule is drawn by hashed lines. Resulting one-dimensional chain in (c) is enclosed by thick solid lines, and the boundary between double-chains is drawn by dotted lines.

C–H···O contact between C(3) and the oxygen atom of the carbonyl group is found in the structure of DBCHep. The central cycloalkanone ring has been found to be significantly distorted (Fig. 8b). The carbonyl group of DBCHep sits at the depression of the central cycloalkanone ring of the neighboring molecule (Fig. 8c). No meaningful contacts between the cycloheptanone rings are found in the structure of MBCHep (Fig. 8d).

Why DBCA Derivatives Tend to Crystallize in a Noncentrosymmetric Form. As already described, a com-

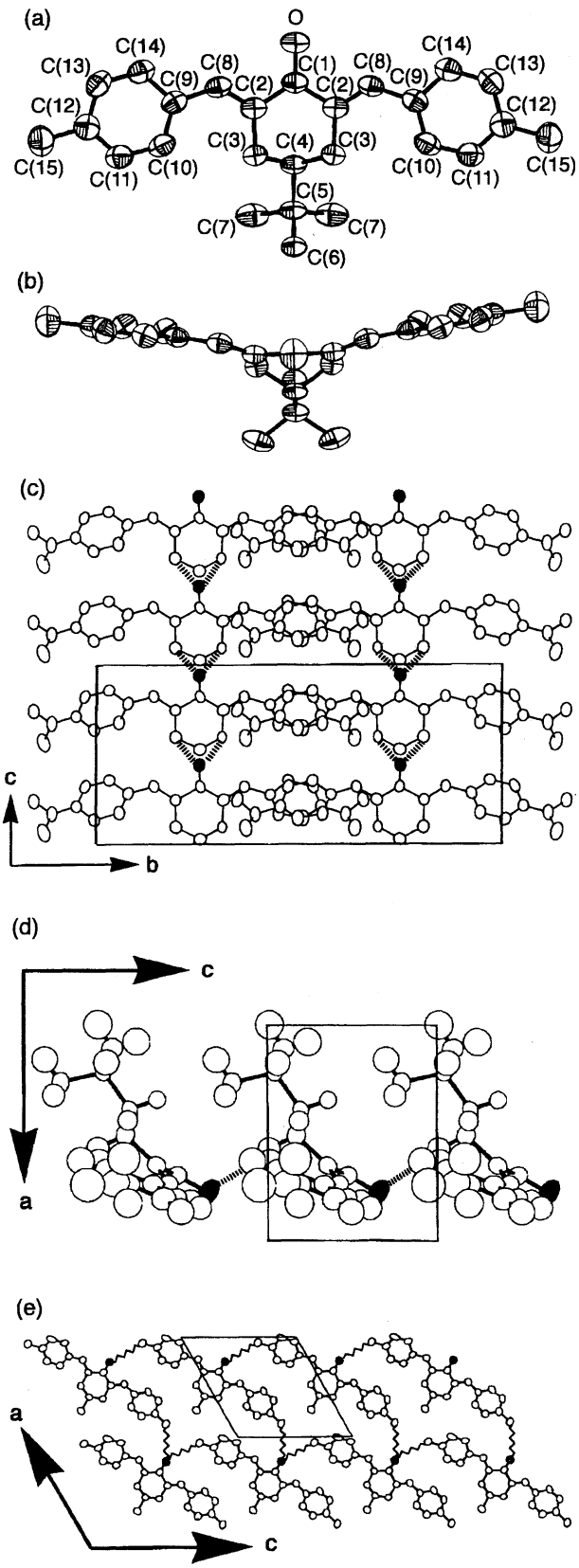

Fig. 7. ORTEP drawing with the atom numbering scheme of MBBCH; view perpendicular to the mean molecular plane (a) and view along the mean molecular plane (b). Crystal structure of DMABCH (c), crystal structure of MBBCH (d), and crystal structure of MBMCH (e). The nearest contact between the carbonyl oxygen and neighboring molecules are drawn by hashed lines or wavy lines.

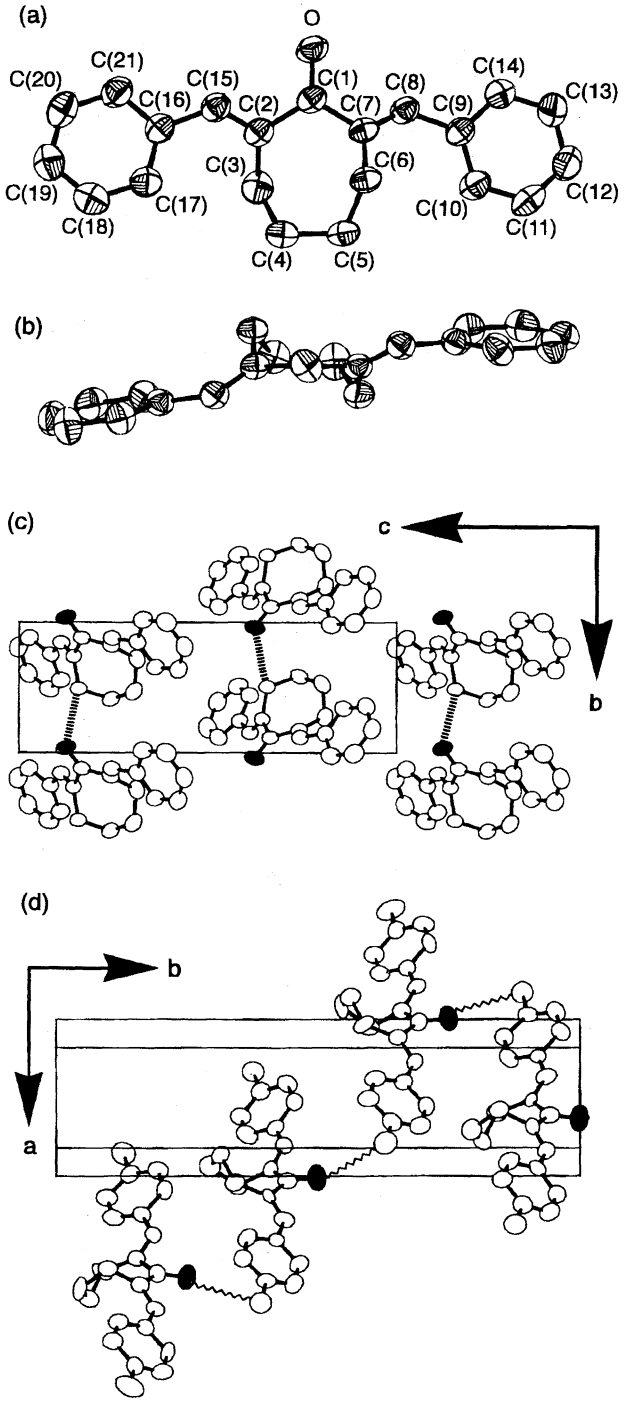

Fig. 8. ORTEP drawing with the atom numbering scheme of DBCHep; view perpendicular to the mean molecular plane (a) and view along the mean molecular plane (b). Crystal structure of DBCHep (c) and crystal structure of MBCHep (d). The nearest contact between the carbonyl oxygen and neighboring molecules are drawn by hashed lines or wavy lines.

mon characteristic found in almost all DBCA derivatives is the existence of a short contact through C(3)–H···O. The distances between the carbonyl oxygen and the nearest non-hydrogen atoms of the neighboring molecule are summarized in Table 6 together with those of related compounds.[25] As

Table 6. Distances Between the Oxygen Atom of the Carbonyl Group and the Nearest Non-Hydrogen Atoms of the Neighbouring Molecule

Compound	Category	Non-hydrogen atom	Distance/Å
DBCP	DBCP	C(3)	3.369(7)
MBCP	DBCP	C(3)	3.30(3)
EBCP	DBCP	C(3)	3.325(6)
MOBCP	DBCP	C(3)	3.342(4)
		C(2)	3.189(4)
BrBCP	DBCP	C(3)	3.286(13)
DBCH[a)]	DBCH	C(3)	3.413
MBMCH	DBCH	C(15)	3.468(10)
MBBCH	DBCH	C(3)	3.690(4)
DMABCH	DBCH	C(3)	3.476(11)
DMABMP[b)]	DBCH	Correspond to C(3)	3.531
DBCHep	DBCHep	C(3)	3.102(2)
MBCHep	DBCHep	C(15)	3.529(15)

a) Ref. 25. b) 3,5-Bis(*p*-dimethylaminobenzylidene)-1-methyl-4-piperidone; Ref. 25.

for MOBCP, the nearest non-hydrogen atom is not C(3), but C(2). This C(2)···O contact appears to be a consequence of an additional electrostatic attraction between C(1) and O. It is clear that there still may be a meaningful C(3)–H···O contact in the crystal of MOBCP (Tables 5 and 6). Table 6 clearly shows that the C(3)–H···O distances can be categorized by the species of the central cycloalkanone ring of the compound.

The C(3)···O distances for all DBCP derivatives are found to be in a narrow range between 3.29 and 3.37 Å. The distances are almost the same as the sum of the van der Waals radius of carbon (1.70 Å) and that of oxygen (1.52 Å).[20]

The values for those DBCH derivatives that have no alkyl substituent at the 4-position of the cyclohexanone ring are longer, i.e., 3.41 Å for DBCH[17] and 3.48 Å for DMABCH. This is simply because the steric hindrance prevents the carbonyl oxygen from approaching the C(3) atoms. Nevertheless, the formation of the similar one-dimensional chains is found in the crystal structures of DBCH and DMABCH. This fact suggests that an attractive force still exists in them. As for the MBBCH, the nearest non-hydrogen atom for the relevant oxygen atom is not C(3), but C(15). As shown in Fig. 7e, when an additional methyl substituent at the 4-position of the central cyclohexanone ring is present, the C–H···O contacts between the cyclohexanone rings are no longer possible.

Interestingly, a trace of the C–H···O hydrogen bond was also found for the 4-*t*-butyl derivative (MBBCH), though the steric hindrance should be much larger than the case for 4-methyl derivative (MBMCH). As can be seen in Fig. 7d, the substituent of this compound does not prevent the oxygen atom from approaching the C(3) atom. The distance (3.69 Å) is the longest value among the DBCA derivatives for which the C–H···O hydrogen bond has been found.

The ability of forming the C–H···O hydrogen bond for DBCH and DBCHep is considered to be weaker than that for DBCP, since their non-planarity of the π-electron system

Table 7. Cutoff Wavelength of the DBCA Derivatives (Methanol Solution)

Compound	Category	Cutoff wavelength/nm
DBCP	DBCP	430
MBCP	DBCP	420
EBCP	DBCP	435
MOBCP	DBCP	440
BrBCP	DBCP	410
DBCH	DBCH	400
MBBCH	DBCH	400
DBCHep	DBCHep	370
MBCHep	DBCHep	400

suggests that the acidity of the concerned hydrogen should decrease in DBCH and DBCHep compared with DBCP. This is also supported from their cutoff wavelengths, as shown in Table 7. Therefore, a short C–H···O contact found in DBCHep is thought to be accidental.

For the DBCA derivatives, the primary factor of cohesion is obviously the dipersion force. If there is a secondary factor of cohesion, such as hydrogen bonds, a CT interaction and so forth, the molecular arrangement is modified so as to satisfy both requirements: molecules tend to be packed as densely as possible (the primary factor), while the specific parts involved in the interaction originating from the secondary factor tend to approach each other as closely as possible. The fact that the C–H···O interaction is found in common for the crystal structures of the DBCP derivatives rather suggests that the interaction is very effective as the secondary factor which determines the molecular arrangement, as suggested for several compounds.[24] It is obvious that more comprehensive studies, such as neutron-diffraction measurements, might be needed to confirm this assertion.

As described, all of the *p*-substituted DBCP derivatives examined form a one-dimensional chain. Concerning the alignment of each chain, two possibilities, i.e., of being parallel or anti-parallel, can be supposed. Although SHG-inactive EBCP forms a double-chain structure, as in the case of MBCP, the bulky terminal chain conformation causes a relationship between the double-chains of EBCP unlike in the case for the SHG-active DBCP derivatives. The fact indicates that the formation of a non-centrosymmetric one-dimensional chain through the C–H···O contacts in DBCPs cannot be a sufficient condition for crystallizing into a non-centrosymmetric form. Yet, the high probability of finding SHG-active crystals for the *p*-substituted DBCP derivatives implies that the formation of a non-centrosymmetric chain is exceedingly advantageous to achieve a bulk non-centrosymmetric arrangement. In fact, in the cases of *o*-, *m*-, and poly-substituted analogues, the oxygen atom of the carbonyl group does not gain access to the C(3)–H moiety, due to a steric hindrance of the lateral substituents. This must be the reason why *o*-, *m*-, or poly-substituted DBCP derivatives do not exhibit SHG activity and their melting temperatures are also low.

For the DBCH derivatives, it is considered that the twisted (bent) molecular conformation primarily contributes to the non-centrosymmetric packing, and that the C–H···O intermolecular interaction also possibly helps it. As for the DBCHep derivatives, the twisted molecular conformation seems to be the reason for the tendency to crystallize in a non-centrosymmetric form.

Conclusion

The correlation between the molecular structure and molecular alignment of DBCA has been examined on the basis of X-ray crystallographic analyses. As a result, a preference for forming a non-centrosymmetric array of molecules has been found, which is led from a stacking of the twisted molecules for the DBCHep derivatives, and from the C–H···O intermolecular interaction and the molecular shape for the DBCP and DBCH derivatives. For the case where the C–H···O interaction cannot be achieved (*o*-, *m*-, and poly-substituted derivatives), the possibility of finding SHG-active crystals is considerably reduced. This implies that the C–H···O interaction plays an important role in determining the non-centrosymmetric molecular arrangement. For molecular crystals, the lattice energy is sometimes found to be substantially unchanged by altering the molecular arrangement, as is found by the phenomenon of polymorphism. Thus, even a weak interaction, like the C–H···O contact, might become a driving force leading to a non-centrosymmetric arrangement preferentially.

References

1) "Nonlinear Optical Properties of Organic Molecules and Polymeric Materials," ed by D. S. Chemla and J. Zyss, Academic Press, San Diego (1987).

2) "Nonlinear Optical Properties of Organic and Polymeric Materials," ed by D. J. Williams, ACS Symposium Series Vol. 233, American Chemical Society, Washington, DC (1983).

3) C. P. Brock and J. D. Dunitz, *Chem. Mater.*, **6**, 1118 (1994).

4) See, for example: "The Merck Index," 11th ed, Merck Inc., Rahway (1989).

5) J. L. Oudar and D. S. Chemla, *J. Chem. Phys.*, **66**, 2664 (1977).

6) J. R. Dyer, "Applications of Absorption Spectroscopy of Organic Compounds," Prentice-Hall Inc., New Jersey (1965).

7) A. I. Kitaigorodskii, "Molecular Crystals and Molecules," Academic Press Inc., New York (1973).

8) H. Yamamoto, S. Katogi, H. Watanabe, H. Sato, S. Miyata, and T. Hosomi, *Appl. Phys. Lett.*, **60**, 935 (1992).

9) J. Kawamata, K. Inoue, H. Kasatani, and H. Terauchi, *Jpn. J. Appl. Phys.*, **31**, 254 (1992).

10) J. Kawamata, K. Inoue, and T. Inabe, *Appl. Phys. Lett.*, **66**, 3102 (1995).

11) J. Kawamata, K. Inoue, T. Inabe, M. Kiguchi, M. Kato, and Y. Taniguchi, *Chem. Phys. Lett.*, **249**, 29 (1996).

12) S. K. Kurtz and T. T. Perry, *J. Appl. Phys.*, **39**, 3798 (1968).

13) G. M. Sheldrick, "SHELX-86. Program for Crystal Structure Determination," University of Gottingen, Germany.

14) A. Altomare, G. Cascarano, C. Giacovazzo, and A. Guagliardi, *J. Appl. Cryst.*, **26**, 343 (1993).

15) P. T. Beurskens, G. Admiraal, G. Beurskens, W. P.

Bosman, S. Garcia-Granda, R. O. Gould, J. M. M. Smits, and C. Smykalla, "DIRDIF. Program for Crystal Structure Determination," University of Nijmegen, The Netherlands.

16) T. Sakurai and K. Kobayashi, *Rep. Inst. Phys. Chem. Res.*, **55**, 69 (1979).

17) R. Taylor and O. Kennard, *J. Am. Chem. Soc.*, **104**, 5063 (1982).

18) G. R. Desiraju, *Acc. Chem. Res.*, **24**, 290 (1991).

19) G. R. Desiraju, *Acc. Chem. Res.*, **29**, 441 (1996).

20) A. Bondi, *J. Phys. Chem.*, **68**, 441 (1964).

21) J. A. R. P. Sarama and G. R. Desiraju, *Acc. Chem. Res.*, **19**, 222 (1986).

22) B. S. Green and G. M. J. Schmidt, *Tetrahedron Lett.*, **49**, 4249 (1970).

23) H. Nakanishi, W. Jones, J. M. Thomas, M. B. Hursthouse, and M. Motevalli, *J. Phys. Chem.*, **86**, 3636 (1986).

24) K. Biradha, A. Nangia, G. R. Desiraju, C. J. Carrell, and H. L. Carrell, *J. Mater. Chem.*, **7**, 1111 (1997).

25) J. Zongchao, J. W. Quail, V. K. Arora, and J. R. Dimmock, *Acta Crystallogr., Sect. C*, **C45**, 285 (1989).